ACS APPLIED MATERIALS & INTERFACES

Research Article

www.acsami.org

Hydrophobic Plasma Polymer Coated Silica Particles for Petroleum Hydrocarbon Removal

Behnam Akhavan, Karyn Jarvis, and Peter Majewski*

School of Engineering, Mawson Institute, University of South Australia, Mawson Lakes, South Australia 5095, Australia

ABSTRACT: In recent years, functionalized hydrophobic materials have attracted considerable interest as oil removal agents. This investigation has applied plasma polymerization as a novel method to develop hydrophobic and oleophilic particles for water purification. 1,7-Octadiene was plasma polymerized onto silica particles using a radio frequency inductively coupled reactor fitted with a rotating chamber. Plasma polymerized 1,7-octadiene (ppOD) films were deposited using plasma power of 40 W and monomer flow rate of 2 sccm, while polymerization time was varied from 5 to 60 min. The surface chemistry of ppOD coated particles was investigated via X-ray photoelectron spectroscopy and time-of-flight secondary ion mass spectroscopy, while Washburn capillary rise measurements were applied to evaluate the hydrophobicity and oleophilicity of the particles. The effectiveness of ppOD coated particles for the removal of hydrophobic matter from water was demonstrated by adsorption of motor oil, kerosene, and crude oil. Petroleum hydrocarbon removal was examined by varying removal time and particle mass. The morphology of oil-loaded ppOD coated particles was examined via environmental scanning electron microscopy observations. Increasing the polymerization time increased the concentration of hydrocarbon functionalities on the surface, thus also increasing the hydrophobicity and oil removal efficiency (ORE). The ppOD coated particles have shown to have excellent ORE. These particles were capable of removing 99.0−99.5% of high viscosity motor oil in 10 min, while more than 99.5% of low viscosity crude oil and kerosene was adsorbed in less than 30 s. Plasma polymerization has shown to be a promising approach to produce a new class of materials for a fast, facile, and efficient oil removal.

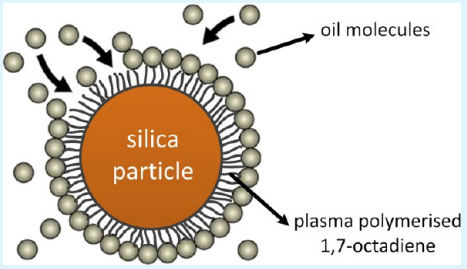

KEYWORDS: *1,7- octadiene, hydrophobicity, oleophilicity, plasma polymerization, water purification*

1. INTRODUCTION

Water pollution has become one of the most serious environmental concerns during the past few decades.[1,2] Oils are among the major pollutants in both drinking water reservoirs and industrial waste waters. Industries producing oil polluted waste waters include metal manufacturing and machining, petroleum refineries, food industry, and other manufacturing plants.[3−5] Contamination of drinking water reservoirs by oils may occur through accidental spills, cracked pipe lines, and runoff of oil from land-based sources.[1,6] The high polluting potential of petroleum hydrocarbons, because of their high persistency and long environmental half-lives, highlights the importance of oil removal from water.[7]

A number of methods are frequently applied for oil−water separation including gravity separation, flotation, chemical coagulation, membrane processes, and adsorption.[8,9] Among these processes, adsorption is becoming more popular as an efficient, easy to use technique that can be feasibly applied in rural areas. The hydrophobic characteristic of oils allows for their adsorption onto a hydrophobic solid via hydrophobic interactions. An ideal oil adsorbent should be highly hydrophobic and oleophilic.[10] The terms "hydrophobicity" and "oleophilicity" refer to water-repelling and oil-wetting properties, respectively.[11] Natural adsorbents such as cotton fibers,[12] zeolite,[13] perlite,[14] fungal biomass,[15] and sugar cane bagasse[16] have been applied for oil removal, but show low efficiency, slow kinetics, and usually adsorb both water and oil.[17,18] Such limitations have led to ongoing research on the development of more efficient synthetic oil adsorbents. Surface modification of organic or inorganic materials has more recently been demonstrated as an effective strategy to synthesize hydrophobic adsorbents for oil removal.[1,19−23] These adsorbents are often rendered hydrophobic via the introduction of polymer functionalities, for example, $-CH_3$[1] and $-CF_3(CH_2)_2$,[23] onto the surface. The highly hydrophobic character of these materials develops a hydrophobic force toward a range of hydrophobic contaminants. Hydrophobic particles have been successfully applied for the removal of spilled oil,[19] organic solvents,[24] and toxic organic compounds[25] from water. Functionalized hydrophobic adsorbents show significant advantages, such as excellent selectivity and fast adsorption kinetics, over natural adsorbent materials.[20]

Plasma polymerization has recently gained increasing interest as a surface modification technique. Plasma, the fourth state of matter, is a partially ionized gas consisting of freely moving electrons, ions, and neutral species with an overall neutral charge.[26] In plasma polymerization, an organic monomer vapor containing specific functional groups is excited into the plasma

Received: May 26, 2013
Accepted: August 13, 2013
Published: August 13, 2013

   dx.doi.org/10.1021/am4020154 | ACS Appl. Mater. Interfaces 2013, 5, 8563−8571

state under the influence of an electric field. The monomer is fragmented into active species via plasma state interactions and is polymerized onto any surface within the reaction chamber.[27] Plasma polymerization is a substrate independent process, and deposited plasma polymers are highly cross-linked and adherent to almost any substrate.[28,29] Such advantages make this technique suitable for surface modification of particles regardless of their geometry, size, and surface chemistry. Deposition of plasma polymers onto particulate surfaces is not however as straightforward as for planar surfaces because of the large surface area which is in contact with plasma.[30] Plasma polymer deposition onto particulate surfaces requires specific types of reaction chambers to efficiently expose particles to plasma and obtain homogeneous coatings. Plasma polymerization reactors equipped with a fluidized bed[30,31] and rotating chambers[32,33] are the two most common designs which have been applied for surface modification of particles. 1,7-Octadiene (OD) is a simple hydrocarbon monomer with an unsaturated structure. This monomer has been widely applied in recent years for deposition of hydrophobic hydrocarbon plasma polymers onto planar substrates.[34−37]

Surface functionalization of hydrophobic adsorbents has been conventionally carried out via wet-chemistry methods. The complexity and substrate dependency of these methods hamper their wide application. Moreover, because of their high rate of waste production, wet-chemistry methods are not environmentally friendly. Applying plasma polymerization for the development of hydrophobic adsorbents is however a green solution to this problem. In contrast to wet-chemistry methods, this technology is simple, substrate independent, and produces virtually no waste.[38]

This research investigates the application of plasma polymerization technology in the development of hydrophobic silica particles for water purification. Plasma polymerized 1,7-octadiene (ppOD) films were deposited onto silica particles to produce hydrophobic hydrocarbon-functionalized particles as schematically illustrated in Figure 1. The aim of this research was to convert low-cost materials into high-value adsorbents. Silica particles were therefore applied as the substrate material since they are inexpensive and commercially available in huge quantities. However, because of the surface independency of plasma polymerization, any other low-cost particles can also be applied as substrates in this technology. Plasma polymerization time was varied from 5 to 60 min to determine its effect on surface hydrophobicity and oil removal efficiency (ORE). The surface chemistry of ppOD coated particles was analyzed via X-ray photoelectron spectroscopy (XPS) and time-of-flight secondary ion mass spectroscopy (ToF-SIMS), while Washburn capillary rise measurement was applied to determine their hydrophobicity and oleophilicity. To evaluate the effectiveness of developed hydrophobic particles in adsorption of hydrophobic matter, oil removal tests were carried out using motor oil, crude oil, and kerosene. Environmental scanning electron microscopy (ESEM) observations were utilized to study the morphology of oil-loaded ppOD coated particles. Surface modification of silica particles by deposition of ppOD films has shown to be an effective method to develop hydrophobic/oleophilic adsorbents for oil removal.

2. EXPERIMENTAL SECTION

2.1. Materials. High-purity grade silica particles with an average size of ∼400 μm and 1,7-octadiene monomer were obtained from Sigma-Aldrich (Castle Hill, Australia). Petroleum ether (analytical reagent 60−80 °C) and light crude oil were obtained from Chem-Supply Pty Ltd. (Adelaide, Australia), while conventional blue dyed kerosene and motor oil were purchased from local stores. The oil viscosities were measured using a rotational viscometer (Fann V-G 35), while their densities were measured using a density meter (Krüss DS7800). Viscosities and densities of oils were measured at a room temperature of (23.0 ± 0.5) °C, and are listed in Table 1. Deionized Milli-Q water was used for oil removal tests. All the materials were used as received without any further purification.

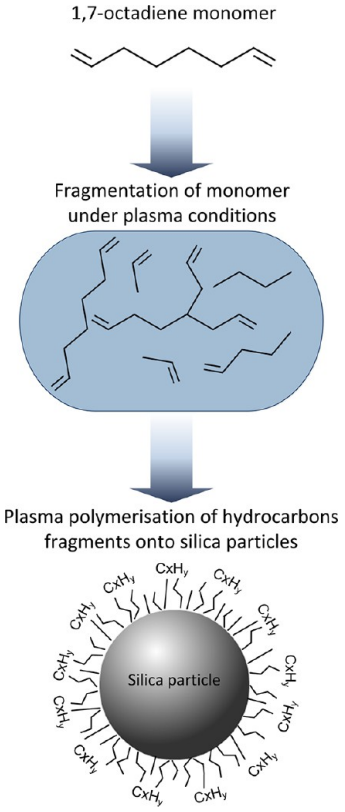

Figure 1. Schematic illustration of 1,7-octadiene plasma polymer deposition onto silica particles.

Table 1. Viscosity and Density of Three Different Oils Used in Oil Removal Experiments

type of oil	density [g/mL]	viscosity [cP]
motor oil	0.89	393
crude oil	0.82	76
kerosene	0.79	2

2.2. Plasma Polymerization. A custom-built inductively coupled rotating plasma polymerization reactor, described previously,[32] was used for plasma polymerization. The reactor was pumped down to approximately 7×10^{-3} mbar using a rotary vacuum pump, while 30 g of dried silica particles were loaded into the plasma chamber. The liquid OD was applied as the precursor monomer followed by at least three freeze−pump−thaw cycles to remove dissolved gases. Plasma polymerization was carried out at constant plasma RF power of 40 W and OD flow rate of 2 sccm, while the polymerization time was varied in the range of 5 to 60 min. A rotation speed of 14 rpm was kept constant for polymerization of all samples.

2.3. X-ray Photoelectron Spectroscopy. The surface chemical composition of uncoated and ppOD coated silica particles was analyzed by XPS using a SPECS SAGE spectrometer. The X-ray source was a nonmonochromatic Mg Kα ($h\nu$ = 1253.6 eV) operated at a power of 200 W (10 kV and 20 mA). A MCD9 electron detector and

dx.doi.org/10.1021/am4020154 | ACS Appl. Mater. Interfaces 2013, 5, 8563−8571

a Phoibos 150 hemispherical analyzer were used for spectroscopy at a takeoff angle of 90°. A pass energy of 30 eV and a resolution of 0.5 eV over the energy range of 0−1000 eV were applied for recording the survey spectra of samples. To correct the effect of charging, all the binding energies were calibrated in reference to the binding energy of aliphatic C 1s component (285 eV). The analysis area was circular and 3 mm in diameter. Calculations of survey elemental compositions were carried out using CasaXPS software while a linear background was applied to all spectra. All XPS analyses were carried out not later than a day after the plasma polymerization.

2.4. Time of Flight Secondary Ion Mass Spectroscopy. ToF-SIMS distribution maps of secondary ions on uncoated and ppOD coated silica particles were obtained using a Physical Electronics Inc. PHI TRIFT V nanoTOF instrument (Physical Electronics Inc., Chanhassen, MN, U.S.A.). The instrument was fitted with a pulsed liquid metal $^{79+}$Au primary ion gun (LMIG), operating at 30 kV energy. An electron flood gun and 10 eV Ar^+ ions provided dual charge neutralization. Base-pressures of 5×10^{-8} mbar or lower were applied for all experiments. "Unbunched" Au_1 instrumental settings were used for obtaining images with high spatial resolutions. SIMS images were obtained from areas of ~450 × 450 μm. ToF-SIMS images were processed and analyzed using WincadenceN software (Physical Electronics Inc., Chanhassen, MN, U.S.A.).

2.5. Washburn Capillary Rise Measurements. The Washburn capillary rise method[39] was applied to measure the water contact angle (WCA) of the uncoated and coated silica particles. A dynamic contact angle meter (DCAT21, Dataphysics) equipped with a Wilhelmy balance and operated by SCAT software was utilized. The Washburn tube (6 cm long, 8 mm inner diameter), packed with 2 g of particles, was placed into close contact with water, and the weight of the water penetrated into the packed bed was recorded as a function of time. By plotting the weight square values (m^2) versus time (t), the water contact angle (θ) was calculated according to the Washburn equation:[39]

$$m^2 = \frac{C\rho^2\gamma_{LV}\cos\theta}{\mu}t \quad (1)$$

Where ρ, μ and γ_{LV} are the density, viscosity, and surface tension of the applied liquid respectively. The capillary constant (C) is a material factor mainly dependent on the porous architecture of the particles.[39] This constant was calculated for each sample using n-hexane as a total wetting liquid, presumably giving a contact angle of 0°. The reported contact angle value of each sample is the average of at least three measurements. The penetration rate of motor oil, kerosene, and crude oil into the packed bed of ppOD coated particles was measured using the same procedure described for water.

2.6. Oil Removal Tests. The oil removal experiments were carried out in batches, at room temperature and at the natural pH of water. Although the solution pH greatly influences the adsorption of ions, it is not a significant factor in the adsorption of hydrocarbons;[16] therefore, the pH of oil−water mixtures were not varied in this study. Initially evaporation tests were carried out for each type of oil to measure the volume of oil which evaporates throughout the experiments. In these tests, 2 g of oil was added to 100 mL of water, and the mixture was subjected to agitation. According to these tests, less than 2% of kerosene evaporated after 15 min of agitation, while no evaporation of crude oil and motor oil was observed.

Oil−water mixtures at a concentration of 20 g/L were prepared by adding 2 g of motor oil, kerosene, or crude oil to 100 mL of water and used for all batch tests. Influence of the hydrophobicity of particles on ORE was investigated by adding 4 g of hydrophobized silica particles, coated at different polymerization times, to the 20 g/L oil−water samples. The suspension was stirred on a magnetic stirrer for 5 min. The influence of removal time on ORE was investigated by adding 4 g of ppOD coated particles (polymerization time = 45 min) to oil−water samples, while varying the stirring time from 30 s to 45 min. Influence of particle mass on oil removal was investigated by adding 1−7 g of ppOD coated silica particles (polymerization time = 45 min) to oil−water samples. This set of experiments was undertaken at optimum removal times of 10 min for motor oil and 30 s for crude oil and kerosene. As observed in Figure 2, agglomerated oil-loaded particles

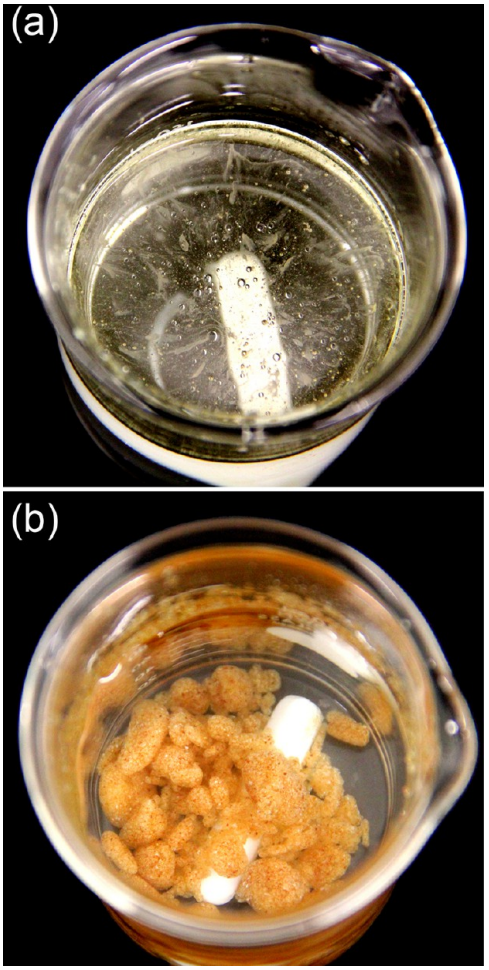

Figure 2. (a) Motor oil−water mixture, (b) motor oil−water mixture treated with ppOD coated particles. (C_i = 20 g/L, removal time = 10 min, particle mass = 50 g/L, plasma polymerization time = 45 min).

settled because of gravity and were therefore easily separable from the effluent using a simple sieve. Agglomerated particles were separated from treated water using a mini sieve (mesh No. = 60). The residual oil was extracted from treated water by adding 100 mL of petroleum ether as a solvent followed by separation via a separation funnel. The concentration of oil dissolved in the solvent was measured using a UV−vis spectrometer (Varian Cary 50). UV−vis absorbance calibration curves were plotted for different wavelengths ranging from 250 to 350 nm. The curves plotted at wavelengths of 300 nm, 320 and 331 nm showed the highest correlation coefficients ($R^2 > 0.9$) for kerosene, crude oil, and motor oil, respectively. The concentrations of oils were therefore determined at these wavelengths. The ORE is calculated by

$$\text{ORE} = \frac{c_i - c_f}{c_i} \times 100 \quad (1)$$

Where c_i is the initial oil concentration and c_f is the concentration of residual oil after treatment. All adsorption tests were conducted in triplicate, and mean values are reported. Standard deviations were less than 2% and 5% of the mean values for OREs higher and lower than 95%, respectively.

2.7. Environmental Scanning Electron Microscopy. Microscopic images of uncoated and ppOD coated silica particles before and after being in contact with oil−water samples were obtained using an environmental scanning electron microscope (FEI Quanta 450 FEG

ESEM). Particles were placed on a cooling stage inside the chamber, and the temperature of the stage was fixed to (2.0 ± 0.5) °C. All the images were captured at a relative humidity of ~18% which was achieved by the introduction of water vapor at a pressure of 130 ± 10 Pa.

3. RESULTS AND DISCUSSION

3.1. Surface Characterization of ppOD Coated Silica Particles. Plasma input power and precursor monomer flow rate define the plasma conditions in plasma polymerization. Our preliminary experiments demonstrated that input power of 40 W and OD flow rate of 2 sccm produced the optimum plasma conditions where the highest surface hydrophobicity is achieved. Plasma polymerization time is however closely linked with the thickness of deposited films and therefore influences the surface properties.[40] To evaluate the influence of polymerization time on surface chemistry and hydrophobicity, plasma power and OD flow rate were kept constant at 40 W and 2 sccm respectively, while polymerization time was varied from 5 to 60 min. From Figure 3, it is clearly visible that with an increase in polymerization time, the atomic concentration of carbon increases. The atomic concentration of carbon increases from ~2% for uncoated silica particles to more than ~70% for silica particles coated at 60 min because of the introduction of hydrocarbon functionalities (C_xH_y) to the surface via deposition of ppOD films. As observed from XPS survey spectra shown in Figure 3, signals originating from the underlying silica substrate are still detected in the sample coated for 60 min. These results indicate that the thickness of ppOD films after 60 min of polymerization is smaller than the sampling depth of XPS which is approximately 8−10 nm.[32]

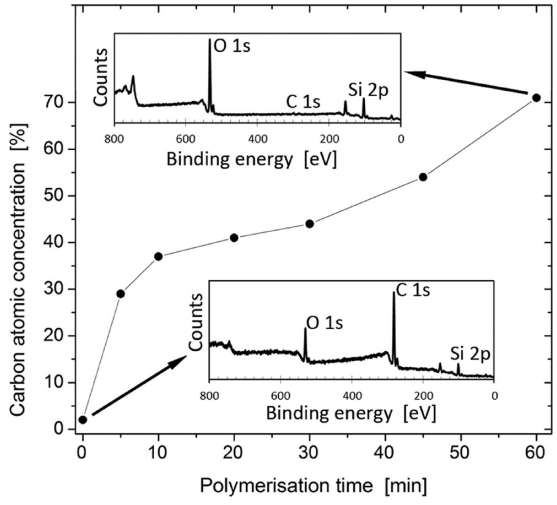

Figure 3. XPS carbon atomic concentration of ppOD coatings as a function of plasma polymerization time. The insets show the representative XPS survey spectra, corresponding to uncoated and ppOD coated silica particles for 60 min.

Deposition of homogeneous hydrocarbon-functionalized coatings onto particles is of particular importance to obtain efficient hydrophobic adsorbents. ToF-SIMS images were applied to evaluate the chemical homogeneity of deposited ppOD coatings. The increase of CH^- counts, recorded at m/z value of 13 amu, versus polymerization time is presented as ion distribution maps in Figure 4. Hydrocarbon functionalities are observed to be evenly distributed across the particle surfaces for all polymerization times. It is also observed that by increasing the polymerization time, the density of CH^- ions increases because of increased deposition of hydrocarbon fragments onto the surface. The increase of CH^- density is however most apparent for polymerization times less than 30 min. This data indicates that at longer polymerization times of 30 min, ppOD films are most likely thicker than the sensitivity depth of ToF-SIMS which is of the order of 1 nm.[41] According to these results and XPS data, the thickness of deposited films after 60 min of polymerization is estimated to be 1−10 nm, which is between the sampling depth of ToF-SIMS (1−2 nm) and XPS (8−10 nm). The uniformity of coatings indicates that the rotating plasma reactor effectively deposits homogeneous hydrocarbon-functionalized films onto particulate surfaces.

Water contact angle (WCA) provides an excellent evaluation of surface hydrophobicity. A more hydrophobic surface has less surface free energy and thus exhibits a higher water contact angle value.[42] WCA of particles were calculated via the Washburn capillary rise method and are listed in Table 2. As observed in Table 2, by increasing the polymerization time the WCA increases from ~36° for uncoated silica particles to more than 90° for silica particles coated for 45 min and longer. Washburn capillary rise measurements are restricted to the calculations of WCA below 90°,[43] thus absolute values of WCA higher than 90° cannot be calculated via this method. Planar glass slides which were coated along with silica particles for 45 and 60 min showed a WCA of (128.5 ± 3.1)° and (143.7 ± 1.8)°, respectively. Although the observed WCAs confirm the highly hydrophobic character of the coatings deposited for

Table 2. Water Contact Angle (WCA) Calculated from Washburn Capillary Rise Method for Uncoated and ppOD Coated Silica Particles

polymerization time [minutes]	WCA [deg.]
uncoated silica	36 ± 3
5	76 ± 1
10	85 ± 1
20	87 ± 1
30	89 ± 1
45	>90
60	>90

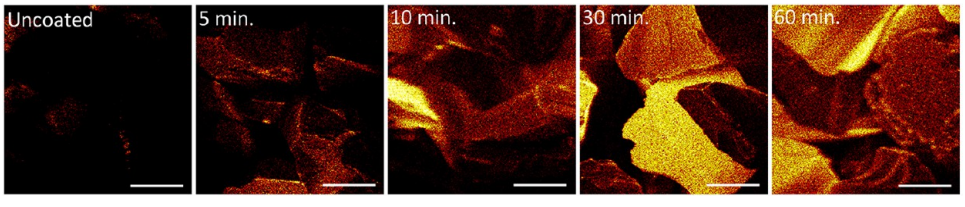

Figure 4. ToF-SIMS CH^- ion distribution maps for uncoated and ppOD coated silica particles (scale bar = 100 μm).

longer than 45 min, they should not be considered as absolute WCAs of particles. WCAs not only depend on the surface chemistry but also on the shape, morphology, and roughness of a surface,[33,44] which are obviously different for the silica particles and glass slides. The increasing hydrophobicity was expected because of the greater carbon concentration on the surface (Figure 3). It is well-known that the surface hydrophobicity inversely correlates with the concentration of polar functional groups on the surface.[45] Silanol groups (Si−OH) are the main polar functionalities present on the surface of uncoated silica particles.[46] By increasing the polymerization time, more polar Si−OH groups are masked by nonpolar C_xH_y fragments, thus producing a more hydrophobic surface. These findings agree with XPS and ToF-SIMS results which suggested significant deposition of hydrocarbon functionalities on silica particles. The highly hydrophobic character of particles coated for 60 min is shown in Figure 5. It is observed that all of the ppOD coated particles float on the interface of water and air, while all of the uncoated silica particles sink in water.

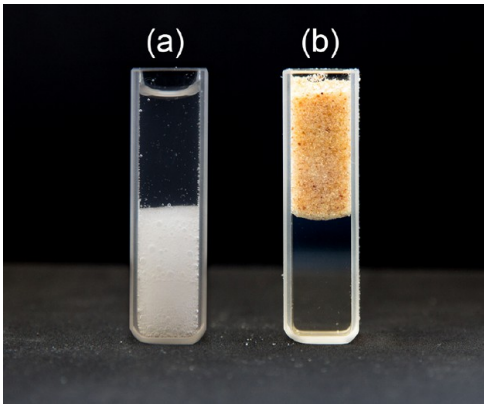

Figure 5. Optical image of (a) uncoated and (b) ppOD coated particles placed on the interface of water and air (plasma polymerization time = 45 min).

Washburn capillary rise measurements not only revealed the hydrophobic character of ppOD coated particles but also demonstrated valuable information on their oleophilic behavior. The penetration rate of water and oils into the packed bed of silica particles was measured to evaluate the hydrophobicity and oleophilicity of the particles, respectively. From Figure 6, the hydrophobic behavior of silica particles coated for 45 min is apparent. Comparing the adsorption curve of an empty tube and that of ppOD coated particles reveals that these particles have not adsorbed any water. On the contrary, ppOD coated particles show strong affinity toward kerosene and crude oil. Such behavior implies that ppOD coated particles are significantly oleophilic. The adsorption kinetics of motor oil is, however, considerably slower than that of crude oil and kerosene. The slow penetration rate of motor oil is attributed to its high viscosity (~ 390 cP). According to the Washburn theory, penetration rate of a liquid into the packed bed of particles is inversely influenced by the viscosity of the liquid.[39] High selectivity and great ORE are the two principal characteristics of an ideal oil adsorbent.[10] Washburn capillary rise measurements revealed that plasma polymerization technology was a successful method to produce particles exhibiting these two characteristics together. The highly hydrophobic and oleophilic properties of ppOD coated

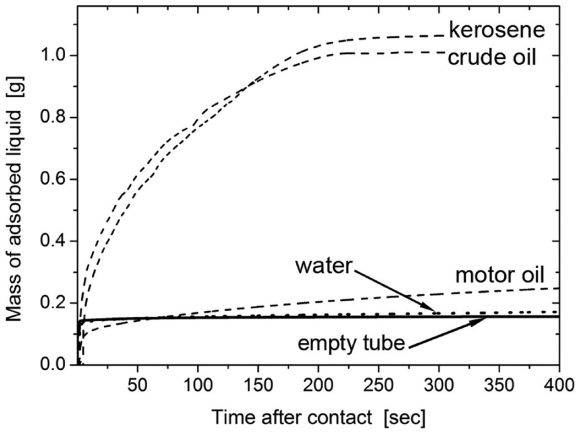

Figure 6. Mass of absorbed water, motor oil, kerosene, and crude oil adsorbed into the packed bed of ppOD coated particles as a function of time after contact in the Washburn capillary rise test. The solid line belongs to the empty test tube. (Plasma polymerization time = 45 min).

particles allow only nonpolar hydrocarbon molecules to be adsorbed onto the surface, while polar water molecules were repelled.

3.2. Influence of Plasma Polymerization Time on ORE.

Oil molecules can be adsorbed onto a hydrocarbon-functionalized surface because of hydrophobic interactions between the petroleum hydrocarbon chains and hydrocarbon groups on the surface.[47] The degree of hydrophobicity of an adsorbent is therefore a crucial factor in removal of hydrophobic molecules from water. The effectiveness of ppOD coated silica particles for removal of hydrophobic matter from water was investigated via motor oil, kerosene, and crude oil removal. As observed in Figure 7, uncoated silica particles do not show a significant

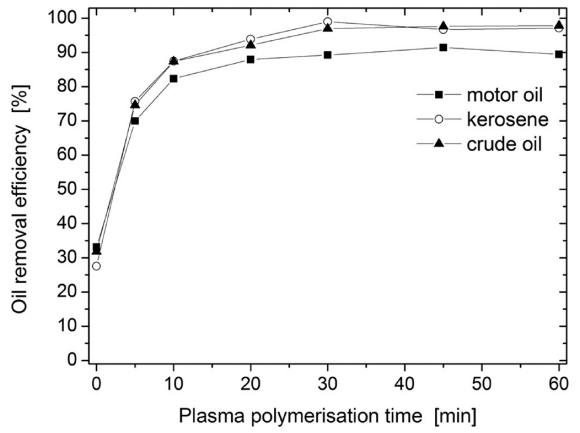

Figure 7. ORE for ppOD coated particles as a function of plasma polymerization time (c_i = 20 g/L, removal time = 5 min, particle mass = 40 g/L).

affinity toward oil molecules and are capable of removing only ~30% of each type of oil from water. While by increasing the polymerization time, the ORE increases and reaches a maximum of ~90% for motor oil and ~99% for both kerosene and crude oil for a polymerization time of 30 min. Such an increase in ORE is due to the deposition of more nonpolar hydrocarbon functionalities on the surface which have produced more hydrophobic surfaces. These results were to be expected and correlate with the variation of both carbon

dx.doi.org/10.1021/am4020154 | ACS Appl. Mater. Interfaces 2013, 5, 8563−8571

concentration (Figure 3) and surface hydrophobicity (Table 2) as a function of polymerization time. This data indicates that tailoring the concentration of hydrocarbon functionalities on ppOD coated particles controls the hydrophobicity of the surface and therefore also controls the magnitude of oil adsorption. Although increasing the polymerization time past 30 min increases the hydrophobicity of particles, it does not significantly affect the ORE. Such behavior suggests that particles exhibiting WCA of ~90° are sufficiently hydrophobic for the adsorption of oils, thus increasing their hydrophobicity beyond 90° does not further enhance the intermolecular hydrophobic interactions. These results also indicate that the thickness of deposited films, which directly influences the hydrophobicity, does not have a significant effect on ORE once the hydrophobicity of particles is sufficiently improved. The influence of oil viscosity on the adsorption process is also demonstrated in Figure 7. The more viscous motor oil exhibited the lowest adsorption for all polymerization times, whereas no significant difference is observed in the adsorption of lower viscosity kerosene and crude oil. Such behavior may be explained by the lower mobility of the more viscous motor oil which inhibits contact of oil and adsorbent.[18] These findings are in accordance with the Washburn capillary rise measurements (Figure 6) that showed an inverse correlation between the oil viscosity and mass of adsorbed oil. Previous research has also reported that the viscosity of the adsorbate is inversely proportion to the ORE.[9,18] According to the obtained results, the maximum ORE is obtained for all three oils at polymerization times of 30−45 min. Silica particles coated at the optimum polymerization time of 45 min were therefore used for time and particle mass variable oil removal experiments.

3.3. Influence of Removal Time on ORE. Time variable oil removal was investigated to determine the kinetics of adsorption and the optimum removal time (t_m) to achieve maximum adsorption. As observed in Figure 8, changes of ORE

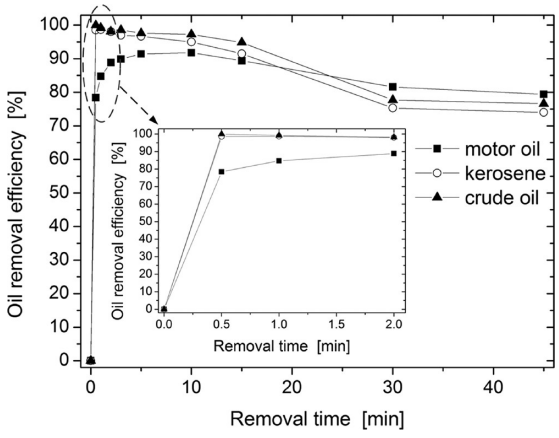

Figure 8. ORE for ppOD coated particles as a function of removal time (c_i = 20 g/L, particle mass = 40 g/L, plasma polymerization time = 45 min).

versus removal time can be divided into two distinct phases: (i) a pure adsorption phase, and (ii) a mixed adsorption/desorption phase. These two phases are respectively defined as areas where the ORE increased and then decreased with increasing removal time. In the pure adsorption phase, the ORE immediately increases with an initial increase in removal time. Such an abrupt increase in ORE can be attributed to the availability of fresh hydrophobic sites on ppOD coated particles resulting in a high driving force for adsorption.[13] The maximum ORE is achieved at $t_m \cong 10$ min for motor oil and at $t_m \cong 30$ s for both crude oil and kerosene. A higher t_m for motor oil may once again be explained by the higher viscosity of this oil. As described earlier, lower mobility of the more viscous motor oil causes insufficient contact of oil and adsorbent thus resulting in longer time to reach maximum adsorption. Once the maximum ORE is achieved, increasing the removal time decreases the ORE, which is attributed to the desorption of oil molecules. As evidenced by our observations from oil removal tests, agglomerated particles loaded with oil break down into smaller agglomerates upon further agitations and oil is thus released back into the water. Collisions of particles at longer agitation times may also cause a mechanical abrasion of adsorbed oil. Simultaneously, desorbed oil molecules may once again be adsorbed onto ppOD coated particles. For removal times greater than 30 min, the ORE does not change significantly. Such behavior may indicate the predominance of a mixed adsorption/desorption mechanism at high interaction times.[9] As observed, the decrease of ORE for longer removal times is more significant for kerosene and crude oil compared to motor oil. The ORE for kerosene and crude oil decreases by ~25% from $t_m \cong 30$ s to t = 45 min, while that of motor oil decreases by ~12% from $t_m \cong 10$ min to t = 45 min. Such a difference suggests that the more viscous motor oil adheres better to the ppOD coated particles. Although higher viscosities decrease the adsorption rate, they may result in stronger hydrophobic interactions. Similar behavior has been observed for the adsorption of high viscosity crude oil onto rubber adsorbents.[48] According to the obtained results, it suggests that the adsorption kinetics of oil onto ppOD coated particles is rapid, particularly for low viscosity oils. Rapid adsorption kinetics correlate with the high oleophilic character of ppOD coated particles demonstrated by Washburn capillary rise measurement findings (Figure 6). The immediate removal of kerosene and crude oil, and slower removal of motor oil from water are also consistent with the results of Washburn capillary rise measurements.

3.4. Influence of Particle Mass on Oil Removal. The influence of particle mass on oil removal was studied by using particle masses of 10−70 g/L, while optimum removal times of 10 min and 30 s were kept constant for motor oil and kerosene/crude oil, respectively. As shown in Figure 9, with an initial increase in particle mass, the ORE for all three oils increases and reaches ~99% for motor oil and more than 99.5% for both kerosene and crude oil. Higher ORE at higher particle masses is simply attributed to more available surface area and thus hydrophobic adsorption sites. Increases in ORE are observed for particle masses of up to 50 g/L for motor oil and 30 g/L for both kerosene and crude oil. Further increases in the particle mass results in the ORE remaining constant. This behavior indicates that once almost 100% of oil is adsorbed, adding excess concentration of hydrophobic adsorption sites does not enhance the magnitude of adsorption. Similar behavior of removal efficiency as a function of adsorbent dose is well documented in the literature.[13,14,49] From Figure 9, it is also suggested that with a constant initial oil concentration, more hydrophobic adsorption sites are required for motor oil removal than for kerosene or crude oil. These results confirm the easier removal of low viscosity oils because of their higher mobility.

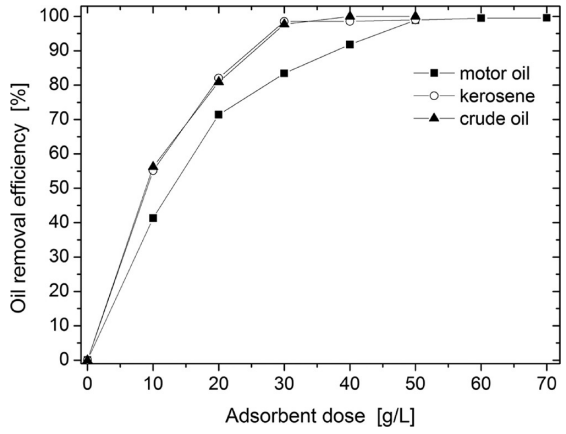

Figure 9. ORE for ppOD coated particles as a function of particle mass (c_i = 20 g/L, removal time for motor oil = 10 min, removal time for kerosene and crude oil = 30 s, plasma polymerization time = 45 min).

In Table 3, the effectiveness of ppOD coated silica particles in petroleum hydrocarbon removal is compared with a number of other adsorbents reported in the literature. As observed, the ppOD silica particles have the highest removal efficiency and fastest removal time among the adsorbents. The relatively low adsorption capacity of ppOD coated particles is attributed to their relatively high density (bulk density ≅ 1.56 g cm^{-3}) compared to other low density adsorbents such as macro-porous carbon nanotubes with a density of 0.015 g cm^{-3}. To compare the effectiveness of developed adsorbents with other adsorbents, ORE should be considered instead of the adsorption capacity. The latter can only provide reliable results if two adsorbents with a same density are compared with each other. The uncoated silica particles show an equilibrium adsorption capacity of 0.16 g/g for crude oil, while that increases by more than 200% to 0.5 g/g via the deposition of ppOD films. Considering that the density of ppOD coated particles remains unchanged, it can be evidently concluded that the plasma polymerization technology is an effective method to remarkably increase the adsorption capacity of silica particles.

3.5. Morphology of Oil-Loaded ppOD Coated Silica Particles. ESEM was applied to visualize the morphology of agglomerated particles which were loaded with adsorbed oil. By using ESEM, it is possible to image samples at higher pressures in comparison to conventional scanning electron microscopes. Owing to both relatively high pressure in the ESEM chamber and reduced temperature of the sample holder, oil droplets do not evaporate into the microscope chamber and can be imaged. No significant difference was observed in the morphology of ppOD particles after being in contact with different oils; thus only representative ESEM images of motor oil-loaded particles are shown here. As observed in Figure 10a, ppOD coated particles do not agglomerate and are distinctly separated from each other. When uncoated silica particles were placed in contact with an oil–water mixture, hydrophobic agglomeration did not occur (Figure 10b). On the contrary, once the ppOD coated particles adsorb oil, they become strongly agglomerated as shown in Figure 10c. As described earlier, such an agglomeration is attributed to hydrophobic interactions between nonpolar hydrocarbon functionalities and hydrophobic petroleum hydrocarbon chains. From Figure 10d, oil droplets trapped in interparticle spaces of agglomerated ppOD coated particles are visible. According to the obtained results, it can be concluded that plasma polymerization is an effective method for the production of hydrophobic adsorbents for a rapid and efficient petroleum hydrocarbon removal.

4. CONCLUSIONS

This study reported a model system to show the potential of plasma polymerization technology in development of a new class of hydrophobic adsorbents. Silica particles were coated by ppOD films at various polymerization times. Plasma polymer coated silica particles were rendered hydrophobic because of deposition of nonpolar hydrocarbon functionalities on the surface. Plasma polymerization time significantly influenced the hydrophobicity and consequently the ORE of ppOD coated particles because of a significant effect on surface chemistry. Surface modified silica particles strongly repelled water while greatly adsorbing oil molecules via hydrophobic interactions. It has been shown that these novel adsorbents can rapidly and efficiently remove three different oils from water. According to the oil removal tests, 99.0–99.5% of the high viscosity motor oil was removed in 10 min of removal time while more than 99.5% of low viscosity crude oil or kerosene were adsorbed in less than 30 s. These developed adsorbents are of direct interest for oil–water separation filters applied in both industrial wastewater treatment and drinking water purification. This novel method could be applied to hydrophobize low cost materials, for example, quartz sand, crushed glasses, and other waste products, to convert them into high value adsorbents.

Table 3. Adsorption Capacity, Removal Efficiency, and Removal Time for Plasma Polymer Coated Silica Particles and a Number of Oil Adsorbents Reported in the Literature

adsorbent	adsorbate	adsorption capacity [g/g]	removal efficiency [%]	removal time	ref.
plasma polymer coated silica particles	motor oil	0.33	>99	10 min	present work
	crude oil	0.5	>99	15 s	
	kerosene	0.5	>99	15 s	
tanned wastes	motor oil	5	98.6	10 min	50
sugar cane bagasse	gasoline	~1.2	94.3	60 min	16
perlite	natural petroleum-contaminated water	0.27	91	100 min	14
walnut shell	standard mineral oil	0.8	83	6 h	15
ionic liquid treated yellow horn shell	crude oil	0.6	not reported	3 h	18
macro-porous butyl rubber	crude oil	23	not reported	5 min	48
magnetic macro-porous carbon nanotubes	diesel oil	56	not reported	30 min	51

dx.doi.org/10.1021/am4020154 | ACS Appl. Mater. Interfaces 2013, 5, 8563–8571

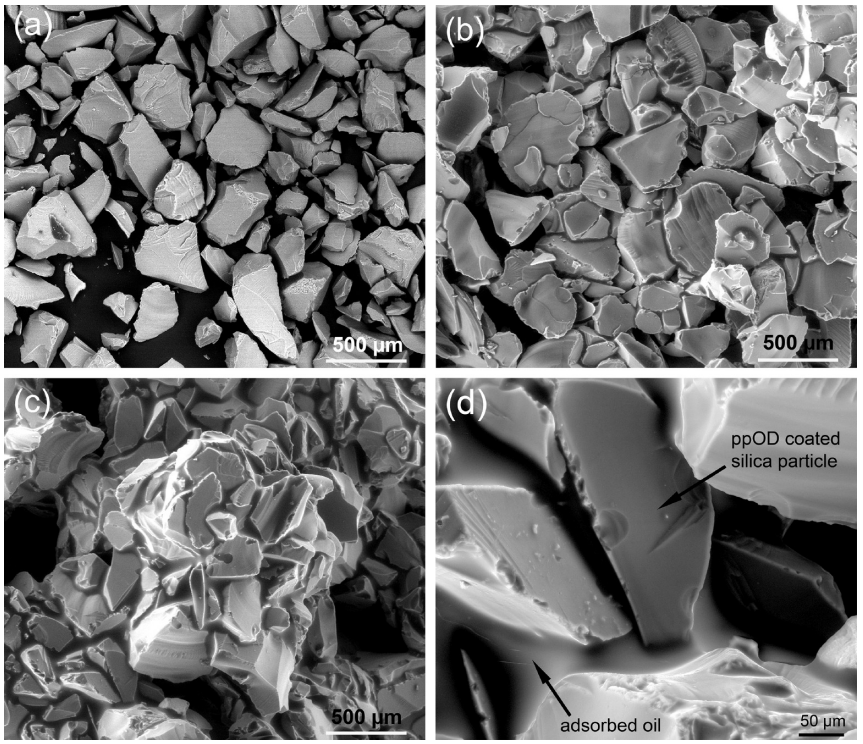

Figure 10. ESEM image of (a) ppOD coated particles, (b) uncoated silica particles after being in contact with oil−water mixture, (c) agglomerated ppOD coated particles after being in contact with oil−water mixture, (d) adsorbed motor oil is visible in between the hydrophobic particles.

Deposition of other functionalities via this technique holds great promise for a fast, facile, and efficient removal of a range of contaminants from water.

AUTHOR INFORMATION

Corresponding Author

*E-mail: peter.majewski@unisa.edu.au. Phone: +61 8 83023162. Fax: +61 8 83023380

Notes

The authors declare no competing financial interest.

ACKNOWLEDGMENTS

The authors gratefully acknowledge the financial support of Government of South Australia, through the Premier Science and Research Fund (PSRF), and National Centre of Excellence in Desalination Australia (NCEDA). The authors acknowledge the facilities, and scientific and technical assistance of the Australian Microscopy & Microanalysis Research Facility at the South Australian Regional Facility (SARF), University of South Australia, a facility that is funded by the University, and State and Federal Governments. We are thankful to Dr. John Denman for undertaking ToF-SIMS, Mr. Stuart McClure for conducting ESEM, and Mr. Alireza Salmachi for viscosity measurements.

REFERENCES

(1) Wang, D.; McLaughlin, E.; Pfeffer, R.; Lin, Y. S. *Sep. Purif. Technol.* **2012**, *99*, 28−35.
(2) Wang, B.; Li, J.; Wang, G.; Liang, W.; Zhang, Y.; Shi, L.; Guo, Z.; Liu, W. *ACS Appl. Mater. Interfaces* **2013**, *5*, 1827−1839.
(3) Friedrich, J.; Unger, W.; Lippitz, A.; Koprinarov, I.; Ghode, A.; Geng, S. H.; Kühn, G. *Compos. Interfaces* **2003**, *10*, 139−171.
(4) Maiti, S.; Mishra, I. M.; Bhattacharya, S. D.; Joshi, J. K. *Colloids Surf., A* **2011**, *389*, 291−298.
(5) Chen, X.; Hong, L.; Xu, Y.; Ong, Z. W. *ACS Appl. Mater. Interfaces* **2012**, *4*, 1909−1918.
(6) Seifi, L.; Torabian, A.; Kazemian, H.; Bidhendi, G. N.; Azimi, A. A.; Charkhi, A. *Water, Air, Soil Pollut.* **2011**, *217*, 611−625.
(7) Guix, M.; Orozco, J.; Garcia, M.; Gao, W.; Sattayasamitsathit, S.; Merkoci, A.; Escarpa, A.; Wang, J. *ACS Nano* **2012**, *6*, 4445−4451.
(8) Srinivasan, A.; Viraraghavan, T. *J. Hazard. Mater.* **2010**, *175*, 695−702.
(9) Deschamps, G.; Caruel, H.; Borredon, M.-E.; Albasi, C.; Riba, J.-P.; Bonnin, C.; Vignoles, C. *Environ. Sci. Technol.* **2003**, *37*, 5034−5039.
(10) Chu, Y.; Pan, Q. *ACS Appl. Mater. Interfaces* **2012**, *4*, 2420−2425.
(11) Zhang, J. L.; Pu, G.; Severtson, S. J. *ACS Appl. Mater. Interfaces* **2010**, *2*, 2880−2883.
(12) Deschamps, G.; Caruel, H.; Borredon, M. E.; Bonnin, C.; Vignoles, C. *Environ. Sci. Technol.* **2003**, *37*, 1013−1015.
(13) Shavandi, M. A.; Haddadian, Z.; Ismail, M. H. S.; Abdullah, N.; Abidin, Z. Z. *Water, Air, Soil Pollut.* **2012**, *223*, 4017−4027.
(14) Moussavi, G.; Bagheri, A. *Environ. Technol.* **2012**, *33*, 1905−1912.
(15) Srinivasan, A.; Viraraghavan, T. *Bioresour. Technol.* **2010**, *101*, 6594−6600.
(16) Brandao, P. C.; Souza, T. C.; Ferreira, C. A.; Hori, C. E.; Romanielo, L. L. *J. Hazard. Mater.* **2010**, *175*, 1106−1112.
(17) Zhu, Q.; Pan, Q. M.; Liu, F. T. *J. Phys. Chem. C* **2011**, *115*, 17464−17470.
(18) Li, J.; Luo, M.; Zhao, C.-J.; Li, C.-Y.; Wang, W.; Zu, Y.-G.; Fu, Y.-J. *Bioresour. Technol.* **2013**, *128*, 673−678.
(19) Zhu, Q.; Tao, F.; Pan, Q. M. *ACS Appl. Mater. Interfaces* **2010**, *2*, 3141−3146.
(20) Choi, S.-J.; Kwon, T.-H.; Im, H.; Moon, D.-I.; Baek, D. J.; Seol, M.-L.; Duarte, J. P.; Choi, Y.-K. *ACS Appl. Mater. Interfaces* **2011**, *3*, 4552−4556.
(21) Deng, D.; Prendergast, D. P.; Macfarlane, J.; Bagatin, R.; Stellacci, F.; Gschwend, P. M. *ACS Appl. Mater. Interfaces* **2013**, *5*, 774−781.

(22) Korhonen, J. T.; Kettunen, M.; Ras, R. H. A.; Ikkala, O. *ACS Appl. Mater. Interfaces* **2011**, *3*, 1813−1816.
(23) Tomina, V. V.; Yurchenko, G. R.; Matkovsky, A. K.; Zub, Y. L.; Kosak, A.; Lobnik, A. *J. Fluorine Chem.* **2011**, *132*, 1146−1151.
(24) Wang, D.; McLaughlin, E.; Pfeffer, R.; Lin, Y. S. *Chem. Eng. J.* **2011**, *168*, 1201−1208.
(25) Perdigoto, M. L. N.; Martins, R. C.; Rocha, N.; Quina, M. J.; Gando-Ferreira, L.; Patrício, R.; Durães, L. *J. Colloid Interface Sci.* **2012**, *380*, 134−140.
(26) Yasuda, H. *J. Polym. Sci.* **1981**, *16*, 199−293.
(27) Jacobs, T.; Morent, R.; De Geyter, N.; Dubruel, P.; Leys, C. *Plasma Chem. Plasma Process.* **2012**, *32*, 1039−1073.
(28) Jama, C.; Delobel, R. In *Multifunctional Barriers for Flexible Structure*; Duquesne, S., Magniez, C., Eds. Springer: Berlin, Germany, 2007; Vol. *97*, pp 109−124.
(29) Vandencasteele, N.; Reniers, F. *J. Electron Spectrosc. Relat. Phenom.* **2010**, *178−179*, 394−408.
(30) Kim, J. W.; Choi, H. S. *J. Appl. Polym. Sci.* **2002**, *83*, 2921−2929.
(31) Karches, M.; von Rohr, P. R. *Surf. Coat. Technol.* **2001**, *142−144*, 28−33.
(32) Jarvis, K. L.; Majewski, P. *J. Colloid Interface Sci.* **2012**, *380*, 150−158.
(33) De Vietro, N.; d'Agostino, R.; Fracassi, F. *Plasma Processes Polym.* **2012**, *9*, 911−918.
(34) Beck, A. J.; Jones, F. R.; Short, R. D. *Polymer* **1996**, *37*, 5537−5539.
(35) Notara, M.; Bullett, N. A.; Deshpande, P.; Haddow, D. B.; MacNeil, S.; Daniels, J. T. *J. Mater. Sci.: Mater. Med.* **2007**, *18*, 329−338.
(36) Deshpande, P.; Notara, M.; Bullett, N.; Daniels, J. T.; Haddow, D. B.; MacNeil, S. *Tissue Eng., Part A* **2009**, *15*, 2889−2902.
(37) Filova, E.; Bullett, N. A.; Bacakova, L.; Grausova, L.; Haycock, J. W.; Hlucilova, J.; Klima, J.; Shard, A. *Physiol. Res.* **2009**, *58*, 669−684.
(38) Yasuda, H.; Matsuzawa, Y. *Plasma Processes Polym.* **2005**, *2*, 507−512.
(39) Chander, S.; Hogg, R.; Fuerstenau, D. W. *Kona Powders Particles* **2007**, *25*, 56−75.
(40) Akhavan, B.; Jarvis, K.; Majewski, P. *Plasma Processes Polym.* accepted for publication.
(41) Vickerman, J. C.; Briggs, D. *ToF-SIMS: Surface Analysis by Mass Spectrometry*; Surfaces Spectra: Manchester, U.K., 2001; p 168.
(42) Gonzalez, E.; Habib, S. B.; Hicks, R. F.; Guschl, P. C.; Gao, L.; Barankin, M. D. *Langmuir* **2009**, *25*, 2495−2500.
(43) Torchinsky, I.; Rosenman, G. *Nanoscale Res. Lett.* **2009**, *4*, 1209−1217.
(44) Chau, T. T.; Bruckard, W. J.; Koh, P. T. L.; Nguyen, A. V. *Adv. Colloid Interface Sci.* **2009**, *150*, 106−115.
(45) Long, C.; Liu, P.; Li, Y.; Li, A. M.; Zhang, Q. X. *Environ. Sci. Technol.* **2011**, *45*, 4506−4512.
(46) Sarawade, P. B.; Kim, J.-K.; Hilonga, A.; Kim, H. T. *Powder Technol.* **2010**, *197*, 288−294.
(47) Kalmykova, Y.; Stromvall, A. M.; Steenari, B. M. *Environ. Technol.* **2008**, *29*, 111−122.
(48) Ceylan, D.; Dogu, S.; Karacik, B.; Yakan, S. D.; Okay, O. S.; Okay, O. *Environ. Sci. Technol.* **2009**, *43*, 3846−3852.
(49) Ghassabzadeh, H.; Mohadespour, A.; Torab-Mostaedi, M.; Zaheri, P.; Maragheh, M. G.; Taheri, H. *J. Hazard. Mater.* **2010**, *177*, 950−955.
(50) Gammoun, A.; Tahiri, S.; Albizane, A.; Azzi, M.; De la Guardia, M. *Environ. Eng. Sci.* **2007**, *6*, 553−559.
(51) Gui, X.; Zeng, Z.; Lin, Z.; Gan, Q.; Xiang, R.; Zhu, Y.; Cao, A.; Tang, Z. *ACS Appl. Mater. Interfaces* **2013**, *5*, 5845−5850.